CHAPTER IV
RESULTS AND DISCUSSION

4.1 Equilibration Time Determination

Prior to measuring the mercury solubility in any solvent, the time for elemental mercury to reach its equilibrium was investigated. *N*-octane was used as a representative for normal paraffins and 2,2,4-trimethylpentane (isooctane) was selected for branched paraffins. Since temperature has an effect on the rate of dissolution (Chang, 1998), in a manner that the lower temperature decreases the rate at which the solute dissolves so that it requires longer time to reach the equilibrium. Temperature at 5°C, which was the lowest temperature in this research, was selected to determine the equilibration time for the whole experiment. The mercury concentration as a function of time in *n*-octane and 2,2,4-trimethylpentane are shown in Figures 4.1 and 4.2, respectively.

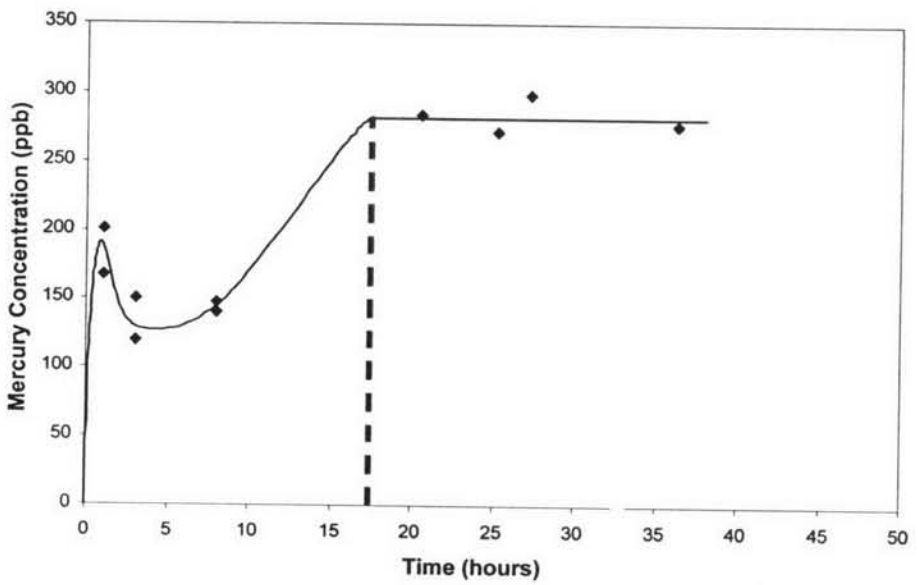

Figure 4.1 Mercury concentration as a function of time in *n*-octane at 5°C.

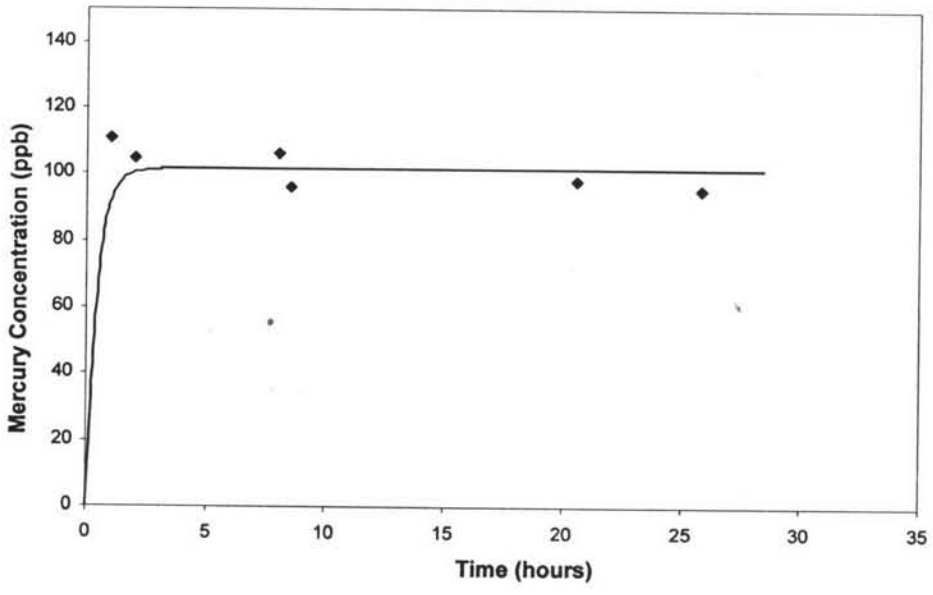

Figure 4.2 Mercury concentration as a function of time in 2,2,4-trimethylpentane at 5°C.

According to Figure 4.1, mercury concentration in *n*-octane rapidly increased in the first hour and then decreased in the next 2-3 hours. After that, it gradually increased again until it reached the equilibrium at 17 hours equilibration, and remained constant at average 280 ppb (wt). This value was identified as an equilibrium concentration of mercury in *n*-octane at 5°C. It is assumed that the abrupt reduction of mercury concentration after the first hour equilibration was due to the adsorption of mercury on the container wall. In this case, the rate of adsorption on container wall may be greater than the rate of dissolution of mercury in *n*-octane. When the container wall was totally equilibrated, the dissolution of mercury in *n*-octane started to increase gradually until it reached its equilibrium. Interestingly, this phenomenon did not occur in 2,2,4-trimethylpentane as illustrated in Figure 4.2. The mercury concentration in 2,2,4-trimethylpentane reached its equilibrium at approximately 100 ppb (wt) after the first hour of equilibration. As the result, to ensure that all solutions for the whole sets of experiments reached their equilibrium, every sample was left equilibrating for at least 20 hours prior to performing analysis step.

4.2 Effect of Mercury Concentration in Headspace and Suspended Mercury on Solubility Study

4.2.1 Effect of Mercury Concentration in Headspace on Solubility Study

Mercury concentrations in vapor phase of *n*-pentane and *n*-hexane at 40°C compared with the mercury concentration in liquid solvent are tabulated in Table 4.1. It can be observed from the result that mercury concentration in headspace was noticeably lower than the mercury concentration in liquid hydrocarbon even at the high temperature (40°C) and the high vapor pressure solvent like *n*-pentane (868 mmHg at 40°C) and *n*-hexane (277 mmHg at 40°C). The average mercury concentrations in vapor and liquid phases of *n*-pentane were 43 ± 2 and 677 ± 11 μg/L, respectively, while the average mercury concentrations in vapor and liquid phases of *n*-hexane were 39 ± 4 and 931 ± 53 μg/L. The percentage of vapor-liquid distribution of mercury concentration, which was calculated from the mercury concentration in vapor phase divided by the mercury concentration in liquid phase, was 6.34% for *n*-pentane and 4.19% for *n*-hexane. It can be inferred that the fraction of mercury in the vapor phase was within the acceptable deviation range for the mercury solubility, which was set to maximum 10% in this experiment. Thus, the headspace over the liquid phase should not have any significant effect on the mercury solubility. Additionally, it can be concluded that the mercury concentration in vapor phase of the other solvents, which the vapor pressure are less than *n*-hexane, should be lower than in the vapor phase of *n*-hexane.

Table 4.1 Comparison between mercury concentration in vapor phase and liquid phase of *n*-pentane and *n*-hexane at 40°C

Solvent	Test No.	Mercury Concentration, µg/L		Vapor-Liquid Distribution of Mercury Concentration (%)
		Vapor phase	Liquid phase	
n-pentane	1	45	689	6.60
	2	42	667	6.33
	3	41	675	6.09
	Average	*43 ± 2*	*677 ± 11*	*6.34*
n-hexane	1	37	957	3.86
	2	36	870	4.13
	3	44	967	4.54
	Average	*39 ± 4*	*931 ± 53*	*4.18*

4.2.2 Effect of Suspended Mercury on Solubility Study

The result from filtration test is shown in Table 4.2. A small difference in mercury concentration between before and after filtering can be noticed. By mean of statistics, three data points of each set are not enough to compare when the two sets of experimental data are evaluated for the significant difference. However, if it was assumed that these six data were in the same set of data, the difference was evaluated based on the average, standard deviation and the coefficient of variation (% CV). The result showed that % CV was 4.58, which was considered within the acceptable deviation range. As the result, it was concluded that the suspended mercury existed in the solution affected on the solubility result within the error range.

Table 4.2 Filtration test of *n*-heptane at 25°C

Test No.	Mercury Concentration, ppb(wt)		Difference ppb(wt)
	Before Filtration	After Filtration	
1	433	406	27
2	409	394	15
3	447	416	31
Average	430 ± 19	406 ± 11	
	418 ± 19, % CV = 4.58		

4.3 Mercury Solubility Study

4.3.1 Single Solvent System

The results on mercury solubility in selected hydrocarbons would be separately described in two sections.

A. Mercury solubility study in 3-methylpentane

Unexpectedly, extremely high concentration of mercury at 9539 ppb (wt) (Table 4.5) was observed during the mercury solubility study in 3-methylpentane at 5°C. The mercury drop appearance was found to change from round and shiny drop (Figure 4.3(a)) to flat and rusty-looked shape (Figure 4.3 (b)). It was obvious that the appearance of mercury drop was different from the normal case. In Figure 4.3(b), a flat drop of mercury in the left vial was obtained from shaking with the shaker at 55 rpm at 5°C, whereas the right vial was shaken vigorously by hand at room temperature and the drop of mercury was further flattening with increasing amount of fine black particles on the mercury surface. As the result, the high surface energy of mercury drop was largely reduced. In addition, fine black particles stuck on mercury drop and the sample container's wall were observed.

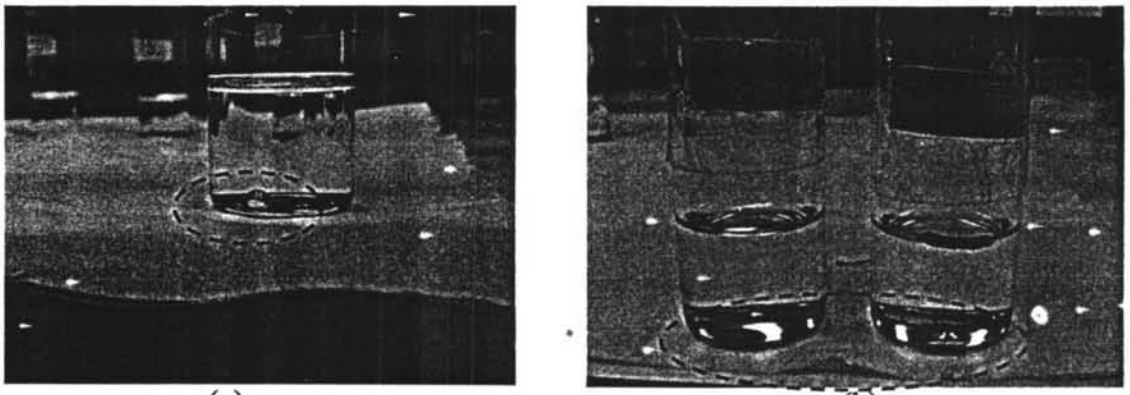

(a) (b)

Figure 4.3 Mercury drop appearance presented in 3-methylpentane (a) normal appearance, round and shiny drop (b) abnormal appearance, flat and rusty-looked drop.

Initially, mercuric sulfide (HgS) formation was assumed possibly due to sulfur impurity in 3-methylpentane. To qualitatively estimate sulfur content in 3-methylpentane, the additional tests were done. The fine black particles were checked for mercury concentration by dissolving with nitric acid (HNO_3), digesting with bromochloride (BrCl), and analyzing by cold vapor atomic absorption spectrometer (CVAAS). The result showed the mercury concentration based on nitric acid solution was minimum 0.16% by weight. The mole equivalent of sulfur in mercury sulfide was calculated and converted to the sulfur concentration as impurity. The obtained sulfide concentration at least 0.05% was checked with the certification of analysis of 3-methylpentane (Appendix D). However, no sulfur was reported. In addition, if sulfur impurity were present in the solvent, the black particle formation would have been limited to the trace amount.

The test of sulfide was further performed to confirm the result. The black particles were treated with warmed 6M hydrochloric acid to liberate H_2S gas. The gas was then tested with a piece of filter paper moistened with lead acetate solution. No black color of lead sulfide (PbS) was observed on the filter paper which indicated a negative sulfide test (Online laboratory tutorials, 2003). Therefore, these black particles were not mercuric sulfide (HgS), but possibly organomercury compound that might occur from the reaction of mercury and 3-methylpentane.

Attempt to re-dissolve the fine black particles was done in different organic solvents that were toluene, dichloromethane, ethanol, methanol, and acetone as their dipole moments are presented in Table 4.3. The 3-methylpentane was drained off the vial while the drop of mercury still remained together with the black particle because large amount of the particles stuck on the mercury drop. Then, the selected organic solvent was added to dissolve the black particles followed by vigorously shaking (by hand) for 10 minutes. The dissolution of black particles and the mercury drop re-appearance were observed. The results are shown in Figure 4.4. In toluene, the solution became clear and the flat and rusty-looked shape of mercury drop resumed its normal appearance. For the other solvents, many small mercury droplets were round shape, but dull appearance especially the mercury drop in methanol and acetone. Additionally, it was noticed that there were many small droplets of mercury, especially in ethanol indicating the change of surface force of mercury which meant the surface tension of mercury was restored and the restoration rate was depended on the property of solvent. According to the dipole moments of solvents listed in Table 4.3, acetone has the highest value while toluene the lowest. The black particles dissolved more quickly in toluene than acetone indicating that the black particles was likely to be non-polar compound.

Table 4.3 Dipole moment value of selected organic solvents (Lange's Handbook of Chemistry, 13th edition, 1987)

Organic Solvent	Dipole Moment (D)
Toluene	0.45
Dichloromethane	1.60
Ethanol	1.69
Methanol	1.70
Acetone	2.88

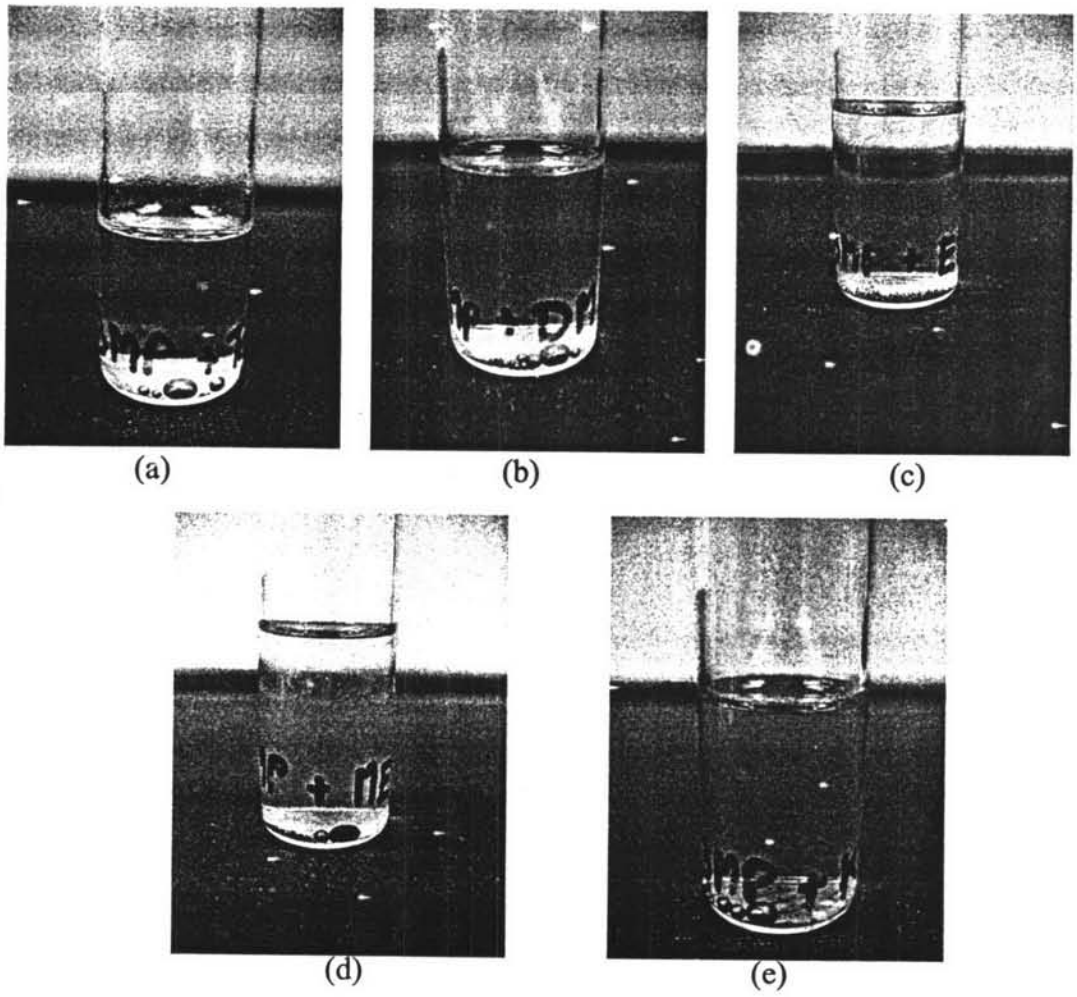

Figure 4.4 Mercury drop appearance in 3-methylpentane after dissolving by solvents (a) Toluene, (b) Dichloromethane, (c) Ethanol, (d) Methanol, (e) Acetone.

The black particles were tested for heat stability. The solid black particles sticking on the drop of mercury inside the vial was heated on a hot plate at various temperatures to observe a change. The pictures of mercury drop appearance before (a) and after (b) heating test are shown in Figure 4.5 and the observation results are described in Table 4.4. Starting from the black particles on a flat mercury mass as shown in Figure 4.5(a), the flat shape of mercury began to show slight shiny surface at the temperature around 60°C. At the temperature around 80°C up to 100°C , the mercury mass gradually shaped up to form a big mercury drop as shown in Figure 4.5(b) and the black particles became yellow and stuck on mercury drop and vial. The cloudy smoke inside the vial was also observed. It was assumed that the black

particles decomposed in the presence of air in the container and the product was mercuric oxide which showed yellow color. However, based on the chemical properties of mercury compound (Aylett, 1973), oxygen and mercury will react on heating to about 350°C to yield mercury (II) oxide (HgO).

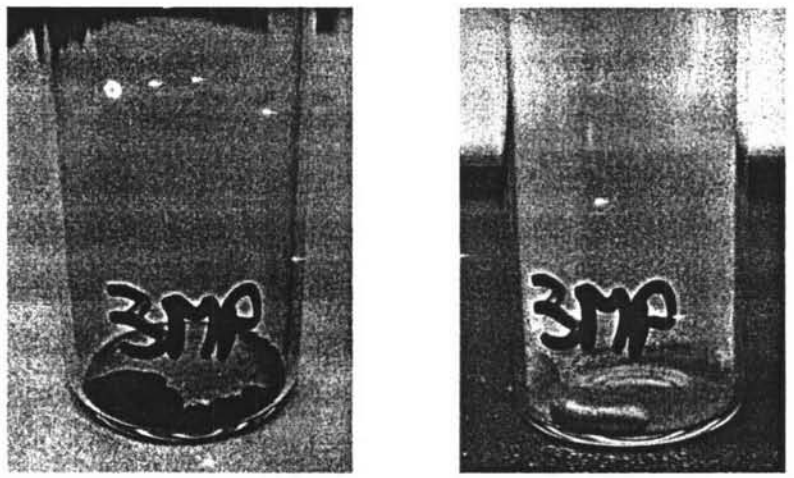

(a) (b)

Figure 4.5 Mercury drop appearance in 3-methylpentane (a) before heating, (b) after heating.

Table 4.4 Change in mercury drop during the heating test

Heating Step	Temperature (°C)	Change in mercury drop appearance
1	28	-
2	40	-
3	56	Flat shape, a little bit shining but still dull.
4	70	Flat shape, a little bit shining but still dull.
5	80	Flat shape but rounder than previous step, a little bit shining but still dull. Fine particles became rust color.
6	90	A little bit rounder, more shining but still dull. Fine particles became rust color.
7	98	A little bit rounder, more shining but still dull. Fine particles became rust color.

According to unexpected behavior of mercury solubility in 3-methylpentane and the preliminary testing, more detailed study is required to identify the black partivles.

B. Mercury solubility study in other solvents

The results on mercury solubility in the other hydrocarbons at the temperature of 5, 15, 25, and 40°C are presented in Tables 4.5-4.8, respectively. The experimental results were also compared with the other study.

Table 4.5 Mercury solubility in hydrocarbons at 5°C

Solvent	Mercury concentration, ppb(wt)			
	Spencer *et al.* (1967)*	Okouchi *et al.* (1981)**	Experimental measurement	
				% CV
n-pentane	-	550	145 ± 12	8.25
n-hexane	569	569	333 ± 25	7.65
n-heptane	556	570	127 ± 7	5.11
n-octane	590	590	285 ± 13	4.60
n-decane	-	-	188 ± 6	3.11
2,2,4-trimethylpentane	374	-	97 ± 8	8.22
3-methylpentane	-	-	9539	-

* Radiotracer technique

** Cold vapor atomic absorption method

Table 4.6 Mercury solubility in hydrocarbons at 15°C

Solvent	Mercury concentration, ppb(wt)			
	Spencer *et al.* (1967)*	Okouchi *et al.* (1981)**	Experimental measurement	
				% CV
n-pentane	-	1016	214 ± 12	5.63
n-hexane	1040	1041	358 ± 13	3.51
n-heptane	1031	1049	159 ± 1	0.25
n-octane	1061	1058	319 ± 18	5.49
n-decane	-	-	245 ± 3	1.04
2,2,4-trimethylpentane	667	-	171 ± 5	2.70

* Radiotracer technique

** Cold vapor atomic absorption method

Table 4.7 Mercury solubility in hydrocarbons at 25°C

Solvent	Mercury concentration, ppb(wt)				
	Kuntz *et al.* (1964)†	Spencer *et al.* (1967)*	Okouchi *et al.* (1981)**	Experimental measurement	
					% CV
n-pentane	1835	-	1839	389 ± 12	3.00
n-hexane	1955	1864	1868	512 ± 11	2.22
n-heptane	-	1872	1891	452 ± 22	4.95
n-octane	-	1869	1844	521 ± 12	2.30
n-decane	1508	-	-	536 ± 13	2.37
2,2,4-trimethylpentane	1166	-	-	361 ± 16	4.32

† Absorption in a Beckman DU spectrophotometer

* Radiotracer technique

** Cold vapor atomic absorption method

Table 4.8 Mercury solubility in hydrocarbons at 40°C

Solvent	Mercury concentration, ppb(wt)			
	Spencer *et al.* (1967)*	Okouchi *et al.* (1981)**	Experimental measurement	
				% CV
n-pentane	-	4315	1027 ± 24	2.31
n-hexane	4313	4327	1392 ± 67	4.83
n-heptane	4412	4412	1216 ± 89	7.32
n-octane	4218	4178	1443 ± 8	0.56
n-decane	-	-	1070 ± 69	6.43
2,2,4-trimethylpentane	2606	-	961 ± 10	1.00

* Radiotracer technique

** Cold vapor atomic absorption method

In addition to the tabulated data, the curves represented the temperature dependence of mercury solubility in the hydrocarbons for this work are illustrated in Figure 4.6.

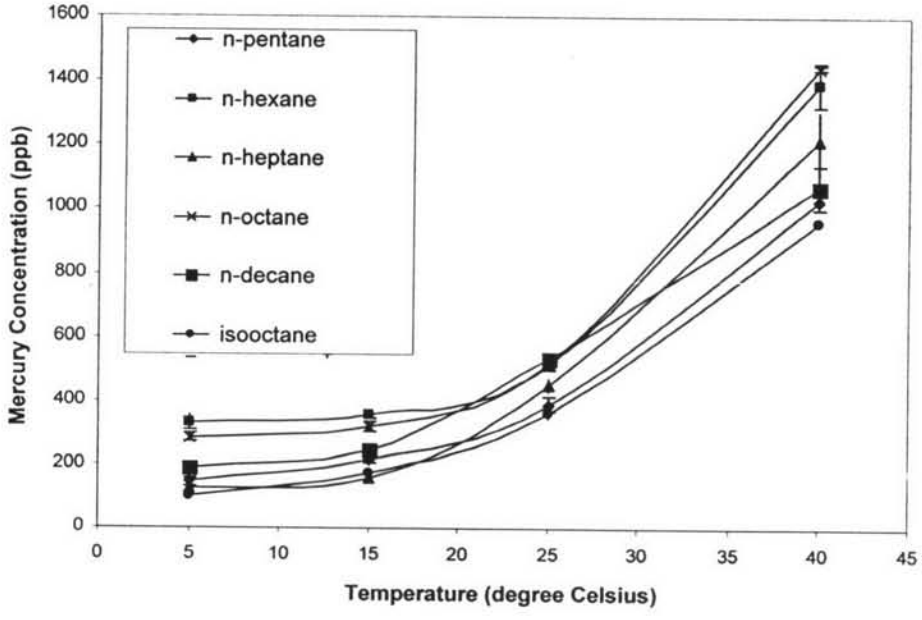

Figure 4.6 Temperature dependence of mercury solubility in hydrocarbons.

In this work, the exponential increase in mercury solubility with temperatures is seen, yet the trend in solubility with carbon atom number for straight chain hydrocarbons was not observed. Additionally, when the solubility of hydrocarbons with the same carbon atom number (n-octane and 2,2,4-trimethylpentane) was determined, it was found that mercury solubility in n-octane was greater than in 2,2,4-trimethylpentane (isooctane) at all studied temperatures. Our results were consistent with the previous reports (Spencer *et al.*, 1967, and Okouchi *et al.*, 1981), which were calculated from the least square equations as described in Appendix C, showed the higher mercury solubility in normal paraffins than in branched paraffin at the same carbon atom number and all temperatures. Considering particularly on normal paraffins, our results showed that the mercury solubility was independent of the number of carbon atoms at low temperature region. Similarly, Clever *et al.* (1987) presented a slight difference in mercury solubility that can be observed at high temperature region but no systematic change in the solubility with the carbon atom number.

A comparison between this work and previous research shows that the solubility data from our experiments were lower as seen, for example, *n*-pentane in Figure 4.7. The large discrepancy may be due to several factors that were applied to the systems such as a method to accomplish the equilibrium (shaking speed and shaking direction), sampling technique, the pre-treatment of hydrocarbon solvents, and the employed analytical method. It was found that shaking manner can strongly influence on the mercury solubility. Mercury concentration in n-pentane could be as high as 1835 ppb (wt) at 25°C when it was vigorously shaken for 20 minutes (Kuntz *et al.*, 1964), while in this work with constant controlling the shaking speed and direction, its concentration was only 389 ± 12 ppb (wt). In addition, the possible source of error e.g. loss of mercury in the headspace was very low compared to the mercury in the liquid phase and the effect of suspended mercury was within the acceptable range as mentioned previously. Therefore, the experimental results were cautiously obtained and valid under this circumstance. However, our results agreed with the trend reported in the literature values (Kuntz *et al.*, 1964, Spencer *et al.*, 1967, and Okouchi *et al.*, 1981).

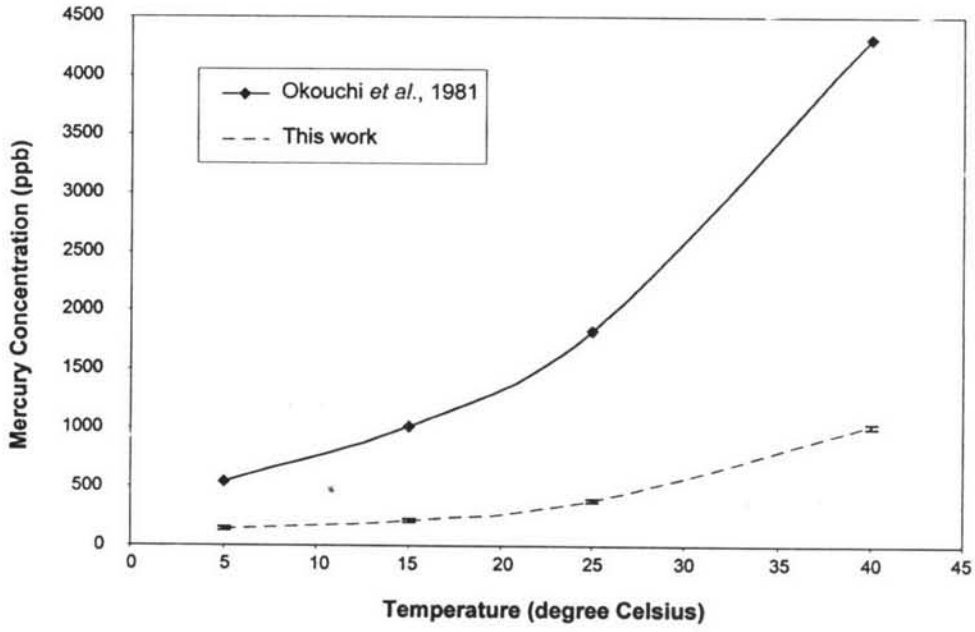

Figure 4.7 Comparison between solubility of *n*-pentane at various temperatures from literature (Okouchi *et al.*, 1981) and this work.

Furthermore, the obtained results were compared with the thermodynamic theory in terms of solubility parameters of the mercury and hydrocarbons. Based on the regular solution and solubility parameters, the trend of mercury solubility in hydrocarbons could be calculated from the values of solubility parameters as mentioned in equations (2.3) and (2.5). The closer the solubility parameters of the solute to the solvent are, the greater the chance of the solute to be more dissolved in the solvent is. Hansen's parameters for mercury and hydrocarbons are tabulated in Table 4.9. It can be seen that the solubility parameters for all selected hydrocarbons consisted of dispersion force component, (δ_d) only and their values slightly increase with carbon atom numbers in case of normal paraffins. However, these differences may be small so that the systematic increasing trend for mercury solubility in normal paraffins with carbon atom numbers could not be observed as shown in other study (Kuntz *et al.*, 1964, Spencer *et al.*, 1967, and Okouchi *et al.*, 1981). For 2,2,4-trimethylpentane, the representative of branched paraffins, the lower mercury solubility than normal paraffin of the same molecular weight (*n*-octane) can be explained by the effect of solubility parameter. As nonpolar hydrocarbon liquids have weak intermolecular attractions to another molecule, these interactions are a

function of the random movement of the electron cloud which is surrounding every molecule. These random movements make the polar fluctuations occur and shift about the surface of molecule so that the numerous temporary dipoles are created constantly, shift about, and disappear. During the time that molecules close together, the random polarities in each molecules tend to induce corresponding polarities in another which result in a play of attraction between molecules. These induced attractions are called "London dispersion forces" or "Induced dipole – induced dipole forces"(Burke, 1984). The surface area of molecule affects to these temporary forces. The larger the molecule is, the greater the intermolecular attractions. Consequently, molecules with straight chains that have more surface area compared to the branched chain molecule of the same carbon atom number have the greater dispersion forces and, finally, the higher solubility parameter. This dispersion forces mean the ability of the solvent to attract mercury atom. The higher the dispersion forces are, the more opportunity the mercury associated and dissolved in that solvent (Burke, 1984). This explained why 2,2,4-trimethylpentane, with lower solubility parameter, had the lesser mercury solubility compared to *n*-octane.

Table 4.9 Hansen's parameters for liquids at 25°C (Barton, 1991)

Liquid	**δ, MPa$^{1/2}$**			
	δ_d	δ_p	δ_h	δ_t
n-pentane	14.5	0.0	0.0	14.5
n-hexane	14.9	0.0	0.0	14.9
n-heptane	15.3	0.0	0.0	15.3
n-octane	15.5	0.0	0.0	15.5
n-decane	15.8	0.0	0.0	15.8
2,2,4-trimethylpentane	14.3	0.0	0.0	14.3
mercury	64.0	0.0	0.0	64.0

4.3.2 Mixed Solvent System : Simulated Condensate

Not only mercury solubility in individual hydrocarbon was conducted, but mixed solvent system, or simulated condensate was also studied. Figure 4.8 illustrated the mercury solubility in simulated condensate and Figure 4.9 showed the mercury solubility in simulated condensate as compared to the mercury solubility in single solvent systems. The thickest line represented mercury solubility in simulated condensate. The normal lines showed mercury solubility in paraffinic hydrocarbons, while the dashed lines showed mercury solubility in cyclic aliphatic and aromatic hydrocarbons (Kittichaichana, 2006). It can be seen that mercury solubility in simulated condensate was located between mercury solubility in individual hydrocarbons. The mercury solubility in the simulated condensate was greater than all paraffinic hydrocarbons, even though the composition of the paraffinic hydrocarbon was accounted for 75%. It was expected that the mercury solubility in simulated condensate might be more or less derivable from the weighted solubility of each hydrocarbon. However, it is apparent from Figure 4.9 and the composition of simulated condensate (Table 3.2) that that is not the case. The solubility of mercury in the simulated condensate was calculated from the empirical correlation as shown in equation 4.1.

$$[Hg]_{simcondy} = \sum_i x_i [Hg]_i \qquad (4.1)$$

where $[Hg]_{simcondy}$ = mercury solubility in simulated condensate

x_i = mole fraction of each components in simulated condensate

$[Hg]_i$ = experimental results for mercury solubility in each components.

Figure 4.10 shows that the mercury solubility obtained from the empirical correlation was lower than the experimental result and the gap between both lines increased with the temperature. It was implied that effect of mixture played important role for predicting the mercury solubility in mixed solvent system. The

mercury solubility in a single paraffin solvent behaved like ideal mixing, while in the mixed solvents especially in the presence of cyclic aliphatic and aromatics behaved like regular mixing solution. To understand the solubility in the condensate, it is recommended to start with the less complicated system such as a binary mixture and ternary mixture and the influence of types of hydrocarbons can be added to match the complexity of the actual condensate.

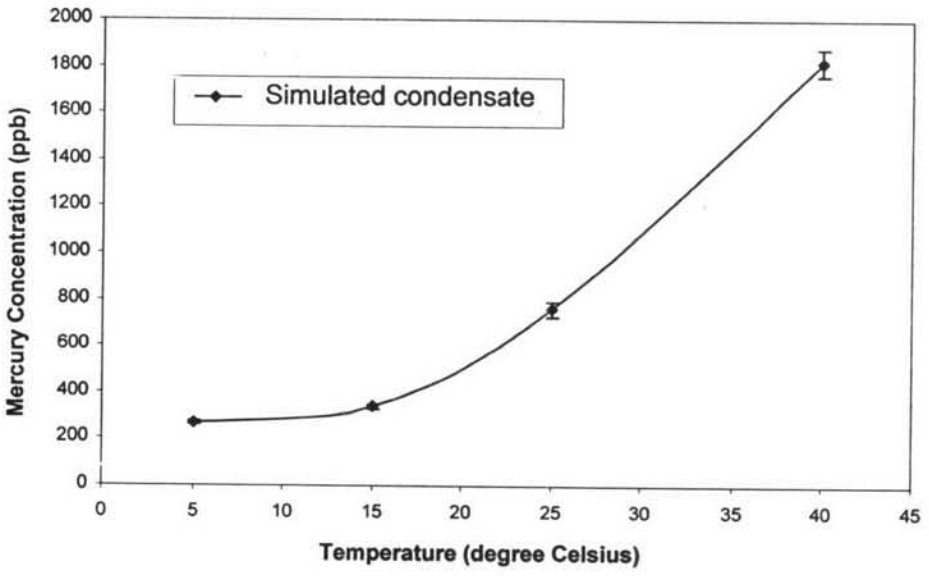

Figure 4.8 Temperature dependence of mercury solubility in simulated condensate.

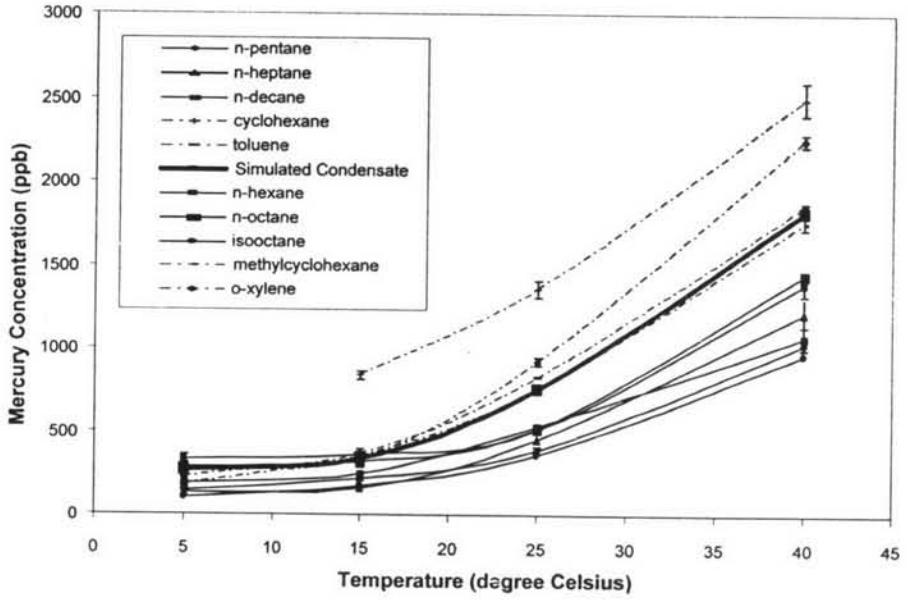

Figure 4.9 Mercury solubility in simulated condensate and single solvent systems.

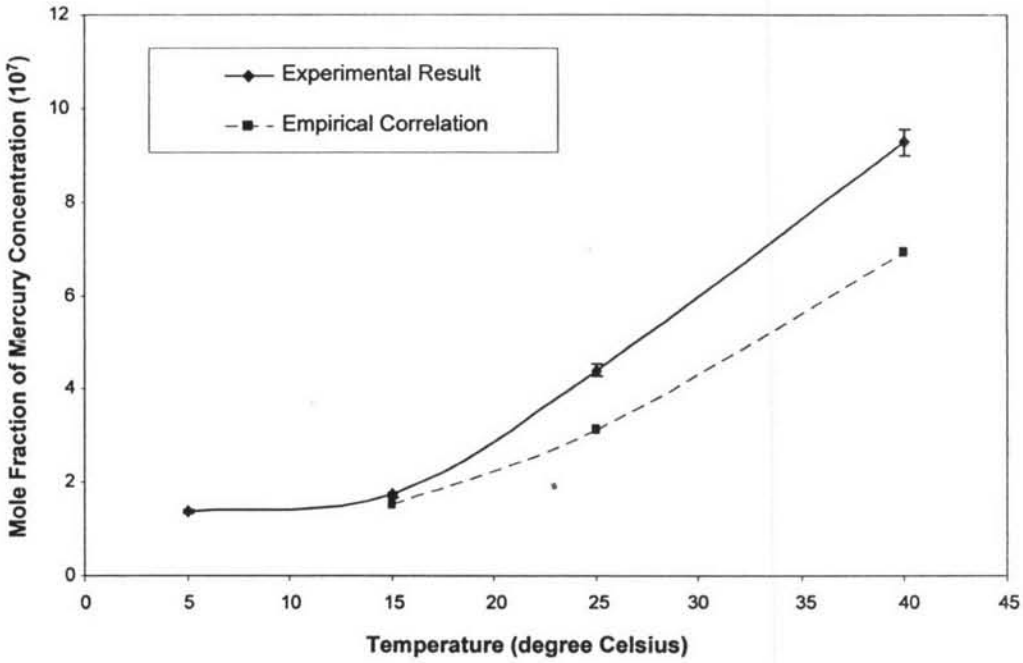

Figure 4.10 Mercury solubility in simulated condensate from experimental result and empirical calculation.

4.4 Hysteresis Study on Mercury Solubility

4.4.1 Single Solvent System

The results of hysteresis study on mercury solubility in the selected hydrocarbons (*n*-pentane, *n*-hexane, *n*-heptane, *n*-octane, *n*-decane, and 2,2,4-trimethylpentane) are illustrated in Figures 4.11 – 4.16.

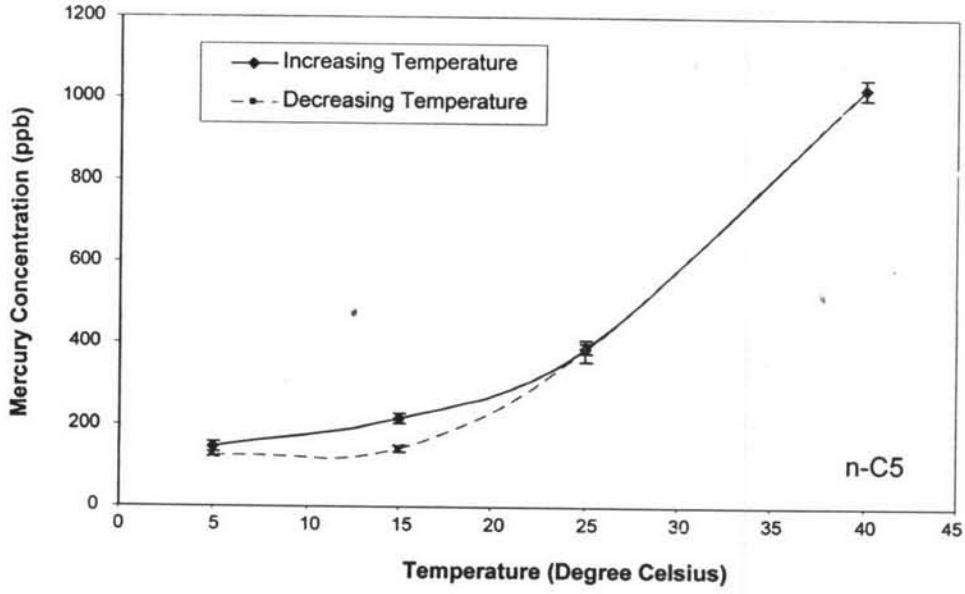

Figure 4.11 Hysteresis study on mercury solubility in *n*-pentane.

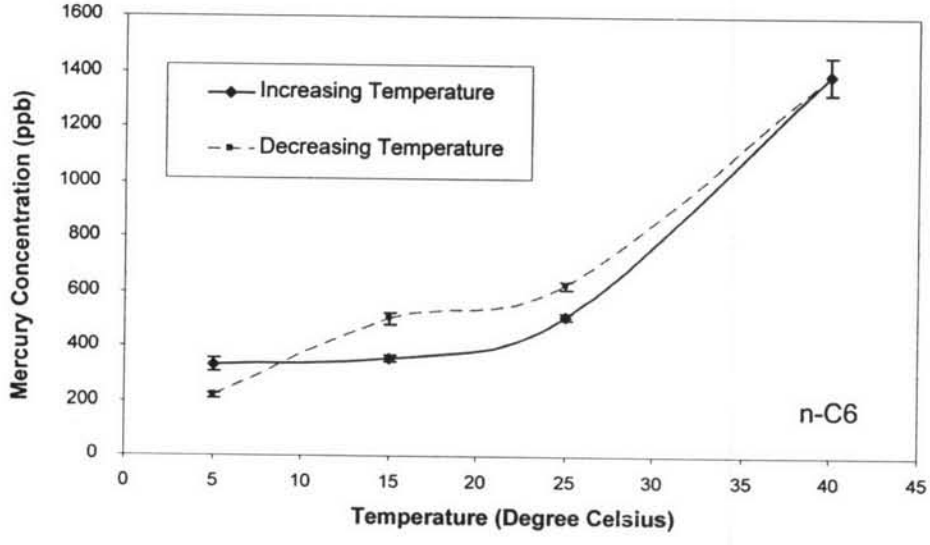

Figure 4.12 Hysteresis study on mercury solubility in *n*-hexane.

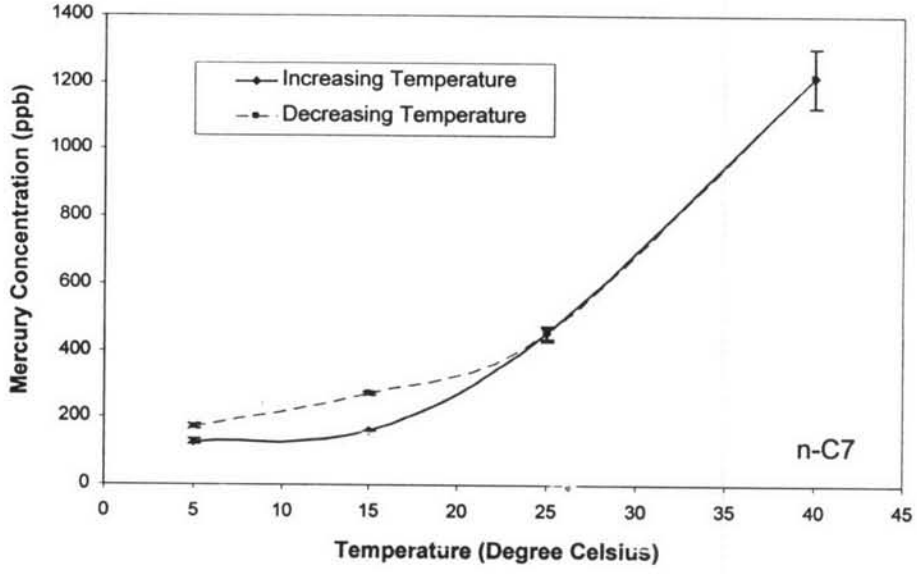

Figure 4.13 Hysteresis study on mercury solubility in *n*-heptane.

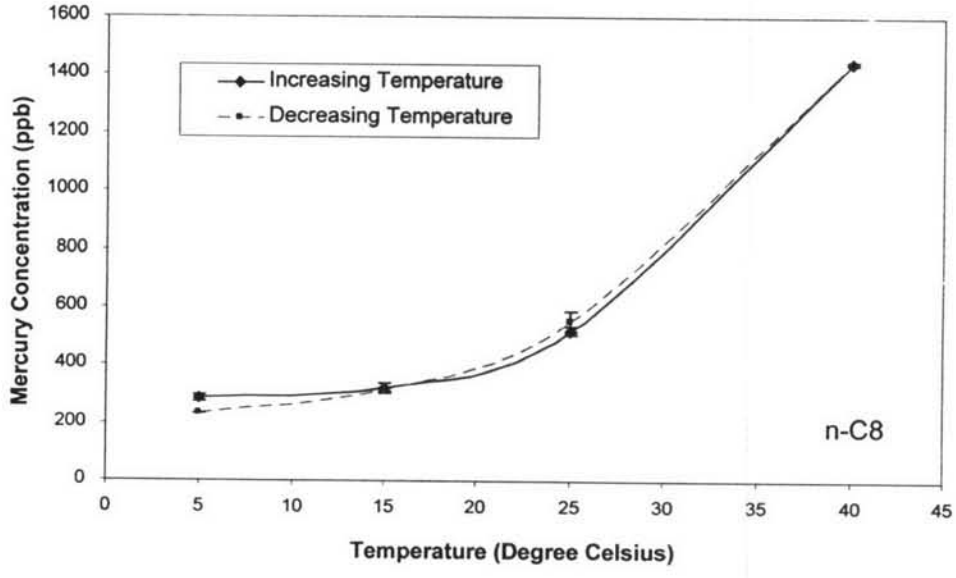

Figure 4.14 Hysteresis study on mercury solubility in *n*-octane.

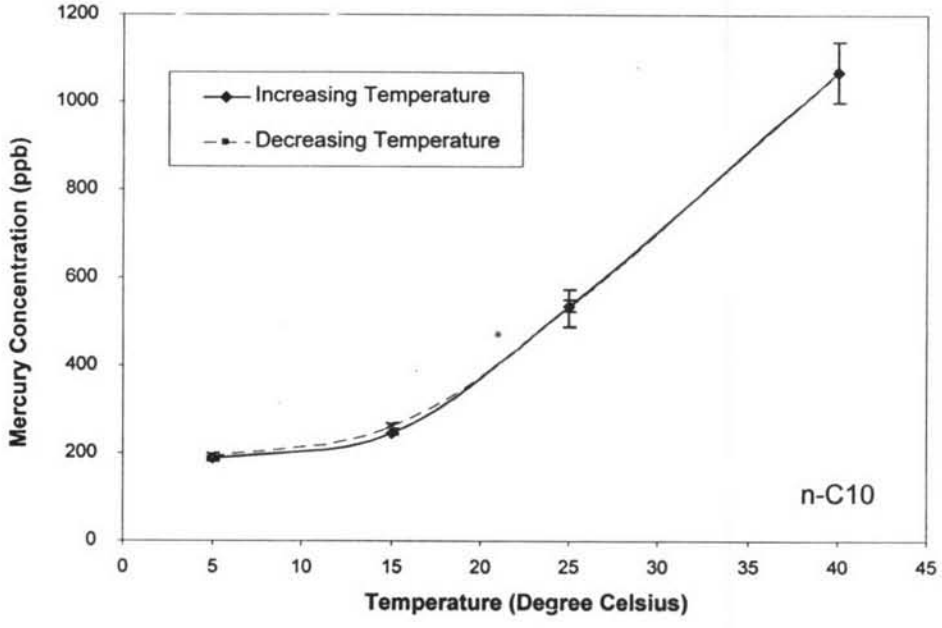

Figure 4.15 Hysteresis study on mercury solubility in *n*-decane.

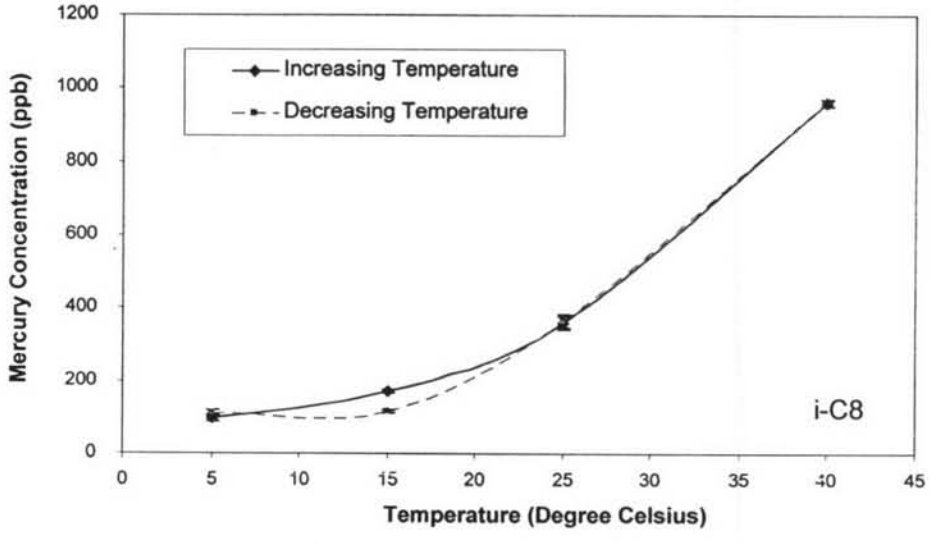

Figure 4.16 Hysteresis study on mercury solubility in 2,2,4-trimethylpentane.

The inconsistency in the obtained results of hysteresis could be noticed. Hysteresis paths of some hydrocarbons showed higher concentration than the solubility curve of the increasing temperature (*n*-hexane and *n*-heptane), lower concentration (*n*-pentane and 2,2,4-trimethylpentane), and close to each other for both increasing and decreasing temperatures (*n*-octane and *n*-decane). Anyhow, the

path differences in mercury concentration for increasing and decreasing temperatures mostly occurred at low temperature region (5-25°C) for all hydrocarbons and the concentration differences were in the range of 5-150 ppb (wt). The interpretations of the experimental data on hysteresis study were done based on several possibilities and assumptions as shown in Figure 4.17. If the hysteresis really existed, the proposed explanations were based on three possibilities, i.e. kinetics of mercury precipitation, molecular association, and/or organomercury formation.

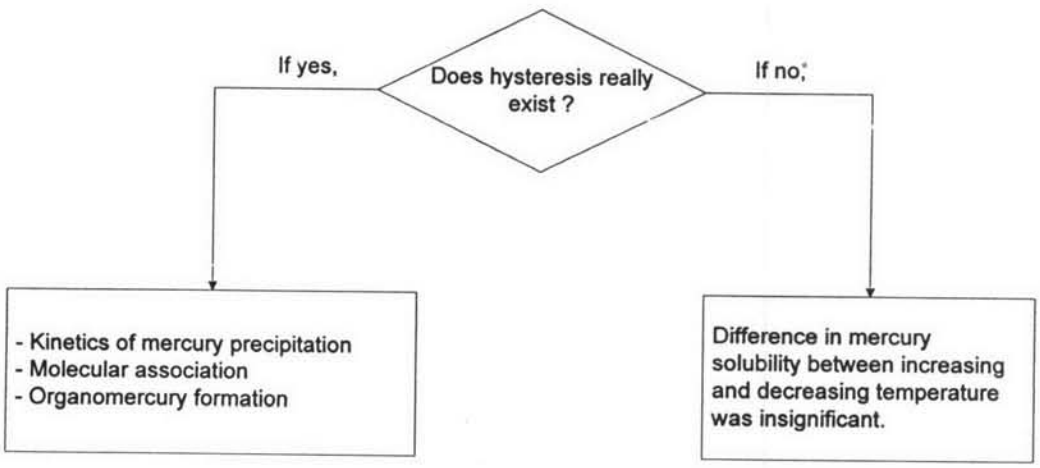

Figure 4.17 Flowchart to determine the hysteresis study on mercury solubility in hydrocarbons.

(1) Kinetics of mercury precipitation

It was suspected that the equilibration time for decreasing temperature (hysteresis study) was different from increasing temperature study (at least 17 hours). If so, the samples for hysteresis study might not be left long enough to reach new equilibrium. In this study, the equilibration time for the whole experiments was based on the study at 5°C as described previously, and at least 17 hours was required for mercury to reach its equilibrium in the hydrocarbons. However, more than 20 hours was used for equilibrating mercury in all hysteresis study, and some solvents were even left longer than 20 hours, while being waited for analysis. For 20 hours equilibration time, the mercury concentration on decreasing temperature would be higher than that of increasing temperature and the hysteresis

path would occur at the low temperature region because it would require longer equilibration time. To prove the assumption, solubility of mercury in the hydrocarbons should be investigated for longer period. If this was true, the gap between mercury solubility on the increasing and decreasing temperature would be taken out.

(2) Molecular association

On decreasing and reaching the equilibrium temperature, mercury atoms associating with hydrocarbon molecules through dispersion force (δ_d) tried to reach equilibrium with the drop of metallic mercury. A mechanism for dissolving process is proposed in Figure 4.18.

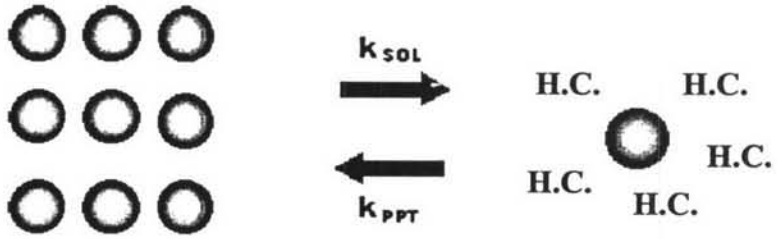

Figure 4.18 Suggested dissolving process for mercury solubility in hydrocarbons.

During decreasing temperature, the equilibrium favors the left side (Figure 4.18). If the rate of precipitation was greater than the rate of dissolution and coupled with the idea of inadequate equilibration time, the lower mercury concentration on decreasing temperature should be observed. On the other hand, if the equilibration was long enough to reach the new equilibrium, the mercury concentration in hysteresis should be located above or the same as the mercury concentration curve obtained from solubility curve of increasing temperature.

(3) Organomercury formation

The formation of organomercury species in hydrocarbon at 40°C was possible since the abnormal solubility of mercury in 3-methylpentane at 5°C was observed. Once the solution was cooled down, the formed organomercury might become stable and govern different precipitation equilibrium from the metallic mercury. The lower mercury concentration in decreasing temperature should be

observed in the experimental result because the re-dissolution process might take longer time. On the contrary, if, again, it was proven that the equilibration was long enough to reach new equilibrium after decreasing temperature, the mercury concentration in the hysteresis curve should have the higher value than mercury concentration in the increasing temperature curve.

In Figure 4.17, if the difference in mercury concentration between the increasing temperature and hysteresis curves was evaluated as insignificance, then the hysteresis did not really exist. The differences for mercury solubility in increasing temperature and decreasing temperature for each solvent and temperature are tabulated in Table 4.10. Since the maximum deviation of the experimental data was less than 10% (Appendix A), the different solubility greater than 10% was considered significant, which indicated the existence of hysteresis. Therefore, the conclusion of the inexistence of hysteresis in *n*-octane and *n*-decane may be possible, whereas the hysteresis existed in the other solvents.

Table 4.10 Differences on mercury solubility between increasing and decreasing temperature

Solvent	Difference on mercury solubility, ppb (wt)*		
	5°C	15°C	25°C
n-pentane	-20	-74	-6
n-hexane	-114	-144	114
n-heptane	44	113	-1
n-octane	-52	-4	34
n-decane	5	19	-6
2,2,4-trimethylpentane (isooctane)	13	-56	3

* Difference on mercury solubility = mercury solubility in decreasing temperature – mercury solubility in increasing temperature.

4.4.2 Mixed Solvent System : Simulated Condensate

The result for hysteresis study in simulated condensate is depicted in Figure 4.19.

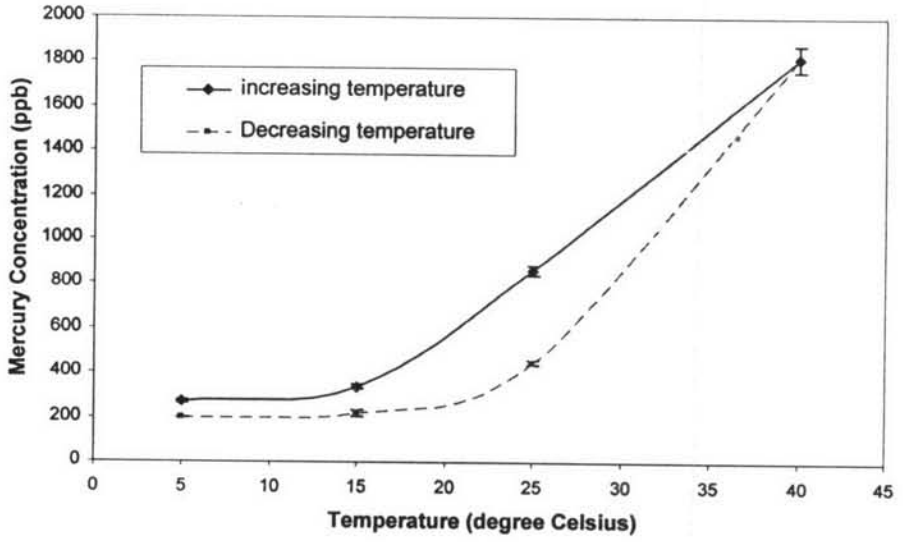

Figure 4.19 Hysteresis study on mercury solubility in simulated condensate.

Hysteresis in mercury solubility was clearly observed. The mercury concentration in hysteresis line was about 400 ppb (wt) lower than in increasing temperature at 25°C. The molecular association and the organomercury formation are two most likely assumptions to explain this phenomenon. However, the effect of the mixture in the regular solution was mainly responsible for the hysteresis as described earlier in the solubility study in simulated condensate.